2019 18th European Control Conference (ECC)
Napoli, Italy, June 25-28, 2019

Analysis of coupled genetic oscillators with delayed positive feedback interconnections

Giulia Giordano[1], Abhyudai Singh[2], and Franco Blanchini[3]

Abstract— **Genetic oscillators have a fundamental role in the regulation not only of intracellular, but also of intercellular functions: for instance, in the segmentation clock, the synchronised oscillation of neighbouring cells generates spatial travelling waves that induce segmentation of precursors of the vertebral column. To investigate this type of phenomena, we consider the behaviour of two genetic negative feedback oscillators, each operating in a different cell, coupled by an intercellular positive-feedback interconnection with delays. The two coupled systems are nominally identical, but can be different due to noise and cell-to-cell variability. When they can be different in general, we study the effect of positive-feedback and of delay in inducing an oscillatory behaviour. When they are identical, we study how the intercellular feedback delay affects the phase difference between the two oscillators.**

I. Introduction

Biomolecular oscillations arise in diverse phenomena, ranging from circadian rhythms [4], [29] to cell-cycle regulation [18] and single-molecule clocks [23]. Several architectures for biomolecular oscillators are possible, all including a negative feedback loop, which is necessary for the onset of sustained oscillations (see [5], [7], [18], [31] and the references therein). Negative-feedback oscillators are the most common [6], [9], [12], [13], [21], but an additional positive feedback can be beneficial to destabilise the system and yield robust oscillations [4], [14], [31], [37]. In many cases, these within-cell oscillations are spatially coupled to their counterparts in neighbouring cells, leading to population-level phenomena, such as synchronisation and travelling waves. Such population-level synchronisation arising from cell-autonomous oscillators has been an intense area of both experimental and theoretical research [15], [26], [34], [38].

Synchronisation of the segmentation clock that operates during vertebrate embryonic development is crucial for the proper formation of the segmented vertebral column [1], [3], [17], [22], [25], [32], [39], [40], [42]. The segmentation clock is implemented by a negative feedback loop, where a key class of proteins (Hes proteins in mouse, and Her proteins in zebrafish) inhibit their own expression. While this intracellular negative feedback yields oscillations within a cell, cell-to-cell coupling based on notch-delta signalling connects neighboring oscillators. This cell-to-cell coupling can be modelled as a delayed intercellular positive feedback loop [25]. This interplay of an intracellular negative feedback loop and an intercellular positive feedback gives rise to spatial travelling waves that lead to segmentation of the precursors of the vertebral column. The phenomenon has been widely studied in zebrafish [2], [11], [27], [28], but is fundamental for somitogenesis in all vertebrates and strongly motivates the study of *coupled genetic oscillators* [16], [24].

Here, we study a system composed of two interconnected genetic oscillators, with two questions in mind. First, we wonder whether non-homogeneity of the two coupled systems promotes or inhibits oscillations: numerical experiments show that both cases are possible, and we investigate the phenomenon to understand when oscillations are favoured and when they are inhibited. Second, when two homogeneous oscillators are interconnected, we study how their phase shift depends on the values of the loop delay.

The contributions of this paper are the following.

- We study the linearisation of a nonlinear model for two coupled genetic oscillators, each based on an intracellular negative feedback, that are interconnected through a delayed intercellular positive feedback (Section II).
- When the two subsystems are heterogeneous, we investigate the role of the intercellular feedback strength and of the delay in the onset of oscillations (Section III). We show that the interconnection can either promote or inhibit oscillations, depending on the delay values and on the relation between the resonance frequencies of the two subsystems.
- When the two oscillators are identical, we give conditions depending on the intercellular feedback delay to ensure that the oscillations are in phase or in phase opposition, based on a regular pattern that depends on the delay (Section IV).

II. Coupling of Two Genetic Oscillators: Nonlinear and Linearised Model

Two coupled genetic Goodwin oscillators [20] can be described by the following nonlinear dynamical system:

$$\dot{m}_1(t) = f(x_1(t), v_2(t)) - \alpha_1 m_1(t) \quad (1)$$
$$\dot{p}_1(t) = \beta_1 m_1(t) - \varepsilon_1 p_1(t) - \zeta_1 p_1(t) \quad (2)$$
$$\dot{x}_1(t) = \varepsilon_1 p_1(t) - \delta_1 x_1(t) \quad (3)$$
$$\dot{m}_2(t) = f(x_2(t), v_1(t)) - \alpha_2 m_2(t) \quad (4)$$
$$\dot{p}_2(t) = \beta_2 m_2(t) - \varepsilon_2 p_2(t) - \zeta_2 p_2(t) \quad (5)$$
$$\dot{x}_2(t) = \varepsilon_2 p_2(t) - \delta_2 x_2(t) \quad (6)$$

where m_i are mRNA concentrations, p_i protein concentrations, x_i active protein concentrations, α_i mRNA degradation rates, β_i protein production rates, ε_i activation rates, while ζ_i

This research was partially supported by the Aspasia grant and the DTF grant awarded to G.G. at the TU Delft.

[1]Delft Center for Systems and Control, Delft University of Technology, The Netherlands. g.giordano@tudelft.nl

[2]Electrical and Computer Engineering, Biomedical Engineering and Mathematical Sciences, University of Delaware, Newark, USA. absingh@udel.edu

[3]Department of Mathematics, Computer Science and Physics, University of Udine, Italy. blanchini@uniud.it

and δ_i are protein degradation rates. The feedback strength is quantified by the Hill function

$$f(x(t), v(t)) = \frac{k_0 + k_1 v(t)}{1 + k_1 v(t) + k_2 x_1^h(t)}$$

with Hill coefficient $h > 0$, where k_0 is related to mRNA transcription rates, k_1 to intercellular positive feedback and k_2 to intracellular negative feedback. Differently from [41], the two systems are coupled by the signals

$$v_1(t) = x_1(t - \tau_1) \quad \text{and} \quad v_2(t) = x_2(t - \tau_2), \tag{7}$$

delayed because a protein from a cell can activate production of the protein in the neighbouring cell only after going through multiple conversion steps that are not instantaneous.

Since f is decreasing with respect to the first argument (and increasing with respect to the second), the intracellular feedback is negative. The intercellular feedback due to delayed signals is instead positive.

The system corresponds to the delayed interconnection of two nonlinear dynamical subsystems (cf. Fig. 1, top), the first with input v_2 and output $y_1 \doteq x_1$, and the second with input v_1 and output $y_2 \doteq x_2$. The state, input and output matrices for the linearised subsystem, $i = 1, 2$, are

$$\begin{aligned} A_i &= \begin{bmatrix} -\alpha_i & 0 & -\phi_i \\ \beta_i & -\gamma_i & 0 \\ 0 & \varepsilon_i & -\delta_i \end{bmatrix}, \quad B_i = \begin{bmatrix} \psi_i \\ 0 \\ 0 \end{bmatrix}, \\ C_i &= \begin{bmatrix} 0 & 0 & 1 \end{bmatrix}, \end{aligned}$$

where $\gamma_i = \varepsilon_i + \zeta_i$, while ϕ_1 and ψ_1 (respectively, ϕ_2 and ψ_2) are the absolute values of the derivatives of $f(x_1, v_2)$ with respect to x_1 and to v_2 (respectively, of $f(x_2, v_1)$ with respect to x_2 and to v_1), computed at the equilibrium.

After Laplace transformation, the transfer function from $v_2(s)$ to $y_1(s)$ is $\tilde{G}_1(s) = \psi_1 G_1(s)$, while the transfer function from $v_1(s)$ to $y_2(s)$ is $\tilde{G}_2(s) = \psi_2 G_2(s)$, where

$$G_i(s) = \frac{\beta_i \varepsilon_i}{(s + \alpha_i)(s + \gamma_i)(s + \delta_i) + \beta_i \varepsilon_i \phi_i} \tag{8}$$

for $i = 1, 2$. Then, for $(i, j) \in \{(1, 2); (2, 1)\}$,

$$\begin{aligned} y_i(s) &= \psi_i G_i(s) v_j(s), & (9) \\ v_i(s) &= e^{-s\tau_i} y_i(s). & (10) \end{aligned}$$

To highlight the intracellular negative feedback loop, we can write the transfer function $G_i(s)$, $i = 1, 2$, as the negative feedback of the transfer function

$$F_i(s) = \frac{\beta_i \varepsilon_i}{(s + \alpha_i)(s + \gamma_i)(s + \delta_i)} \tag{11}$$

and the feedback coefficient ϕ_i, as shown in Fig. 1, bottom. We can also define $u_1(s) = \psi_2 v_1(s)$ and $u_2(s) = \psi_1 v_2(s)$, so that the coupled oscillators are described by the following relations in the Laplace domain:

$$\begin{aligned} y_i(s) = G_i(s) u_j(s) &= \frac{F_i(s)}{1 + \phi_i F_i(s)} u_j(s), & (12) \\ u_i(s) &= \psi_j e^{-s\tau_i} y_i(s). & (13) \end{aligned}$$

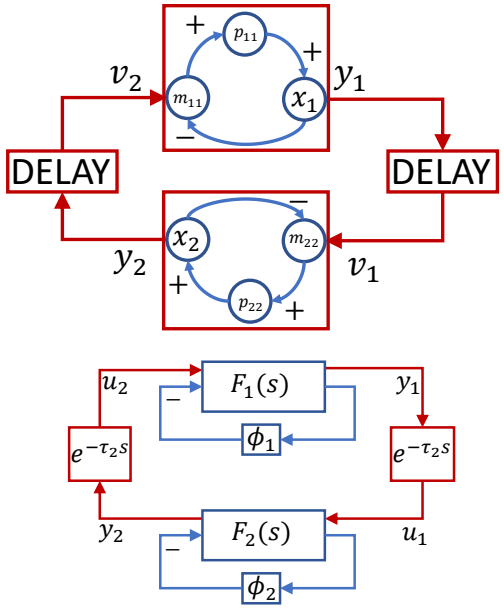

Fig. 1: **Two coupled genetic oscillators.** Top: two negative (intracellular) feedback loops coupled by a positive delayed (intercellular) feedback loop. Bottom: block diagram with the negative loops of transfer functions F_i and ϕ_i and the positive loop with delays $e^{-\tau_i s}$.

with $(i, j) \in \{(1, 2); (2, 1)\}$. Equivalently, we can write:

$$y_i(s) = F_i(s) \left(-\phi_i y_i(s) + \psi_i e^{-s\tau_j} y_j(s) \right), \tag{14}$$

with

$$F_i(s) = \frac{\beta_i \varepsilon_i}{(s + \alpha_i)(s + \gamma_i)(s + \delta_i)}. \tag{15}$$

III. Role of Intercellular Feedback and Delays in Yielding Oscillations

The two coupled subsystems are nominally identical: they represent oscillations occurring in identical cells belonging to the same population. However, biologically this is unlikely to be perfectly satisfied, due to noise and cell-to-cell variability.

Hence, we consider two *possibly non-homogeneous* subsystems and we investigate *the effect of the positive feedback interconnection on their oscillatory behaviour*. As observed in simulation, coupling can have an unpredictable effect on oscillations, which can be either promoted or inhibited. Here, we explain why we can have these two possible outcomes.

In the absence of the positive feedback loop (i.e., when $\psi_1 = \psi_2 = 0$), the characteristic polynomials of the two (decoupled) subsystems are:

$$p_i(s) = (s + \alpha_i)(s + \gamma_i)(s + \delta_i) + \beta_i \varepsilon_i \phi_i, \ i = 1, 2. \tag{16}$$

When $\psi_1, \psi_2 \neq 0$, the characteristic equation is

$$p(s) - \kappa e^{-s\tau} = 0, \tag{17}$$

where

$$\begin{aligned} p(s) &= p_1(s) p_2(s), & (18) \\ \kappa &= \beta_1 \beta_2 \varepsilon_1 \varepsilon_2 \psi_1 \psi_2, & (19) \\ \tau &= \tau_1 + \tau_2. & (20) \end{aligned}$$

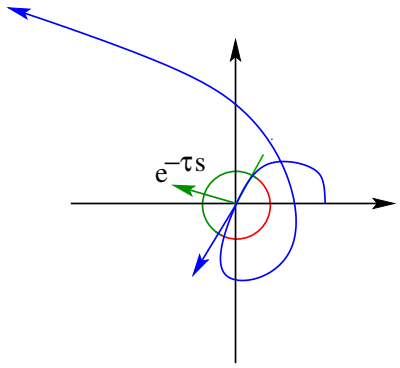

Fig. 2: **Nyquist diagram** of the polynomial $p(j\omega)$ (blue curve), with its tangent vector at the point where $p(j\omega) = 0$ (blue arrow). Favourable directions are in the green half circle, unfavourable directions in the red half circle.

To mathematically formulate our question, we assume that: **(I)** the first subsystem has one negative real pole and two purely imaginary poles, $p_1(j\bar{\omega}) = p_1(-j\bar{\omega}) = 0$ for some $\omega > 0$;
(II) the second subsystem is stable: $p_2(s)$ is Hurwitz.
The first subsystem is in its "limit oscillatory conditions", i.e. its linearisation has purely imaginary eigenvalues associated with oscillatory modes, and we wish to see whether interconnecting it with the second subsystem inhibits or promotes oscillations. We consider favourable an interconnection that leads to oscillatory instability, which is fundamental, e.g., for embryonic development in the segmentation clock.

Definition 1: Given $\tau = \tau_1 + \tau_2$, the positive feedback interconnection is:

- *favourable* if there exists a gain κ^* such that, for any gain κ with $0 \leq \kappa \leq \kappa^*$, the two imaginary roots of the interconnected system transit to the complex right half plane, hence the system becomes unstable, while all other roots remain stable (with negative real part);
- *unfavourable* if there exists a gain κ^* such that, for any gain κ with $0 \leq \kappa \leq \kappa^*$, the two imaginary roots of the interconnected system transit to the complex left half plane, hence the system becomes stable.

An interconnection can be either favourable or unfavourable, depending on τ and $\bar{\omega}$.

Let us first visualise our main idea with the help of Fig. 2. Consider the Nyquist diagram of the polynomial

$$p(j\omega) = p_1(j\omega)p_2(j\omega), \tag{21}$$

which is the blue curve in Fig. 2, at the point $\bar{\omega}$, where $p(j\omega) = 0$. The vector tangent to the Nyquist diagram at this point is

$$\frac{dp(j\omega)}{d\omega} = j\frac{dp(j\omega)}{d(j\omega)} = jp'(j\omega), \tag{22}$$

represented in Fig. 2 as the blue arrow.

Now, consider the green half circle centered in zero with radius 1, which is on the opposite side with respect to the concavity of the Nyquist diagram, and the complementary red half circle, on the same side as the concavity. We can observe that, when the positive feedback loop is added, the Nyquist diagram of $p(j\omega)$ is shifted in the direction of $-e^{-j\bar{\omega}\tau}$. Then:

- if $e^{-j\bar{\omega}\tau}$ is in the green half circle, then the interconnection is favourable, because the diagram is locally shifted to not encircle the origin.
- conversely, if $e^{-j\bar{\omega}\tau}$ is in the red half circle, then the interconnection is unfavourable, because the diagram is locally shifted to encircle the origin.

We can also look at how the roots of the closed-loop polynomial

$$p(s) - \kappa e^{-\tau s} \tag{23}$$

vary depending on κ. The closed-loop polynomial has the root $\lambda(\kappa)$ such that $\lambda(0) = j\bar{\omega}$. The expression

$$p(\lambda(\kappa)) - \kappa e^{-\tau\lambda(\kappa)} = 0 \tag{24}$$

gives us the root λ as an implicit function of k. Then, we can consider the derivative of $\lambda(\kappa)$ with respect to κ, computed at $\kappa = 0$:

$$\left.\frac{d\lambda(\kappa)}{d\kappa}\right|_{\kappa=0} = -\left.\frac{-e^{-\lambda(\kappa)\tau}}{p'(\lambda) + \kappa\lambda(\kappa)e^{-\lambda(\kappa)\tau}}\right|_{\kappa=0} = \frac{e^{-j\bar{\omega}\tau}}{p'(j\bar{\omega})}. \tag{25}$$

For the interconnection to be favourable, the root $\lambda(\kappa)$ must move towards the right half plane. Hence, the phase of the derivative must satisfy the relation

$$\underline{\angle \frac{e^{-j\bar{\omega}\tau}}{p'(j\bar{\omega})}} = \underline{\angle e^{-j\bar{\omega}\tau}} - \underline{\angle p'(j\bar{\omega})} \in (-\frac{\pi}{2}, \frac{\pi}{2}), \tag{26}$$

corresponding to the inequalities

$$-\frac{\pi}{2} < \underline{\angle p'(j\bar{\omega})} - \bar{\omega}\tau < \frac{\pi}{2}. \tag{27}$$

A. Fast and slow critical system

Another qualitative reasoning, useful for design purposes, can be discussed with the help of Fig. 3, for delay values that are negligible with respect to the period: $\tau_1, \tau_2 \approx 0$.

Let us denote by *critical system* the first subsystem $G_1(s)$ with the imaginary poles. Assume that the *non-critical system* $G_2(s)$, instead, is stable with a negative real pole and a pair of complex poles with negative (but small in absolute value) real part. Assume that, in both cases, the real pole is much larger in magnitude than the pair of complex poles. Then, the qualitative behaviour of the transfer function $G_2(s)$ (*non-critical* system) can be seen in Fig. 3, top panel, which shows its Bode diagram. The magnitude of the transfer function has a peak corresponding to the frequency associated with the pair of complex poles. At that frequency, the phase of the transfer function quite abruptly decreases from zero degrees to -180 degrees (it will further decrease to -270 degrees after the frequencies associated with the real pole). On the other hand, the transfer function $G_1(s)$ of the *critical* system has a resonance peak corresponding to the frequencies of the oscillatory (purely imaginary) poles. The behaviour of the closed-loop system, in the presence of the positive feedback interconnection, will be different depending on whether the critical system is slower or faster than the non-critical system. We denote an oscillatory system

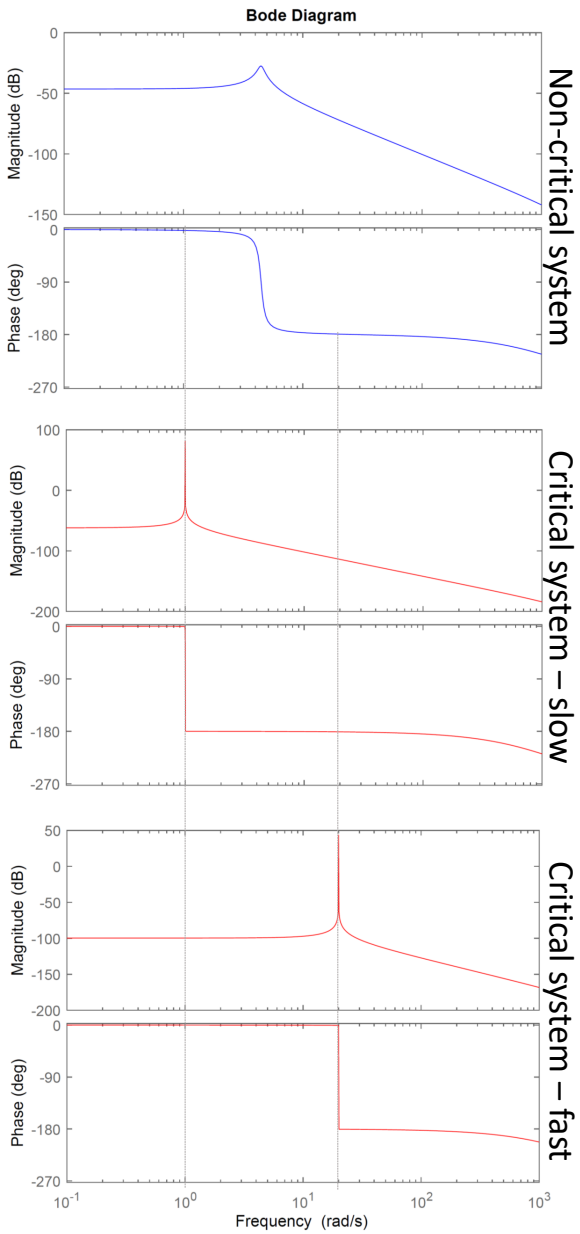

Fig. 3: **Bode diagrams of the transfer functions:** G_2 as in (28), is the non-critical system (blue, top panel); G_1^{slow} as in (29), is a slower critical system (red, central panel); G_1^{fast} as in (30), is a faster critical system (red, bottom panel).

as slow (respectively, fast) if its resonance peak occurs at low (respectively, high) frequencies. Then, if the critical system is slow, and in particular if the magnitude of its complex poles is smaller than the magnitude of the complex poles of the non-critical system, the situation is the one depicted in Fig. 3, central panel: the resonance peak of the oscillatory system $G_1(s)$ occurs when the phase of the transfer function $G_2(s)$ is zero. Therefore, when we close the loop, the critical system "sees" a positive gain with a zero phase, hence an overall positive gain, which suppresses oscillations. Conversely, if the critical system is fast, and in particular if the magnitude of its complex poles is larger than the magnitude of the complex poles of the non-critical system, then the situation is the one depicted in Fig. 3, bottom panel: the resonance peak of the oscillatory system $G_1(s)$ occurs when the phase of the transfer function $G_2(s)$ is -180 degrees. Therefore, when we close the loop, the critical system "sees" a positive gain with a -180 degree phase, hence an overall negative gain that favours sustained oscillations. In particular, in Fig. 3, the top panel shows the Bode diagram of the transfer function

$$G_2(s) = \frac{143}{s^3 + 1501s^2 + 770s + 30000}, \tag{28}$$

the central panel shows the Bode diagram of the transfer function

$$G_1^{slow}(s) = \frac{1}{s^3 + 1250s^2 + s + 1250}, \tag{29}$$

and the bottom panel shows the Bode diagram of the transfer function

$$G_1^{fast}(s) = \frac{10}{s^3 + 2400s^2 + 400s + 960000}. \tag{30}$$

To summarise, when the delays are small, having a faster critical system is favourable for oscillations, while having a slower critical system is unfavourable. The analysis can be generalised to the case of non-negligible delays: the outcome depends on whether the delay is closer to an even, $2k\pi/\omega$ ($k \in \mathbb{N}$), or odd, $(2k+1)\pi/\omega$ ($k \in \mathbb{N}$), multiple of the semi-period π/ω.

IV. Syncronisation for Identical Oscillators: Phase-Shift Patterns

Here we study the effect of the intercellular delay on the synchronisation between the two coupled genetic oscillators, assumed to be equal (which is nominally the case).

When the two subsystems are exactly equal, both p_1 and p_2 in the previous section have the root $j\bar{\omega}$, hence $p'(j\bar{\omega}) = 0$. Then the buttonhole in Fig. 2 becomes a cusp and the theory becomes more involved. We do not investigate this case in detail, for space reasons. However, we stress that it is always possible to find a value of the negative feedback ensuring that the individual system is an oscillator. Then, if the two oscillators are equal, the resulting oscillations will have the same frequency and it is very interesting to look at the resulting phase shift.

The main question now is how the positive feedback can induce synchronisation. We provide a qualitative insight based on heuristic arguments, which is then corroborated by simulation results. With the support of Fig. 1 (bottom), we can make the following observations.

- For each oscillator, if there are permanent sustained oscillations, the phase shift between u_2 and y_1 (respectively, between u_1 and y_2) is $-\pi$.
- Accordingly we expect that, in the absence of the delays ($\tau_1 = \tau_2 = 0$), assuming that the two oscillators have limit cycles (of the same frequency), the coupling due to intercellular positive feedack yields a stable limit circle with y_1 and y_2 in phase opposition, namely with a phase shift equal to $-\pi$. This happens because the signal u_2

arrives in phase with the local negative feedback signal $-\phi_1 y_1$ (respectively, u_1 arrives in phase with $-\phi_2 y_2$).
- The fact that the signals $-\phi_1 y_1$ and u_2 are in phase (respectively, $-\phi_2 y_2$ and u_1 are in phase) excites the oscillations.

How does the phase shift change when the delay is non-zero? First consider the case in which

$$\tau_1 = \tau_2 = \frac{\tau}{2}. \tag{31}$$

With a heuristic approach, we consider the first harmonic of the oscillations. Assume that the period is $T = \frac{2\pi}{\omega}$, and let the first harmonic of the first oscillator be

$$y_1(t) = \mu \sin(\omega t). \tag{32}$$

The second oscillator is

$$y_2(t) = \mu \sin(\omega t + \Delta), \tag{33}$$

where either $\Delta = 0$ (in phase), or $\Delta = \pi$ (in phase opposition). The signal received by the first oscillator is

$$y_2^{shift}(t) = \mu \sin[\omega(t - \tau_1) + \Delta]. \tag{34}$$

Between the two options $\Delta = 0$ or $\Delta = \pi$, it is chosen the one that enables $y_1(t)$ and $y_2^{shift}(t)$ to be as much as possible in phase opposition, namely the one that minimises

$$\begin{aligned}\int_0^T y_1(t) y_2^{shift}(t) dt &= \int_0^T \mu^2 \sin(\omega t) \sin[\omega(t-\tau_1)+\Delta] dt \\ &= \cos(-\omega\tau_1 + \Delta) \int_0^T \mu^2 \sin(\omega t)^2 dt \\ &= \mu^2 \frac{\pi}{\omega} \cos(-\omega\tau_1 + \Delta),\end{aligned}$$

where we used the facts that $\sin(\omega(t-\tau_1)+\Delta) = \sin(\omega t)\cos(-\omega\tau_1+\Delta) + \cos(\omega t)\sin(-\omega\tau_1+\Delta)$ and that $\int_0^T \sin(\omega t)\cos(\omega t) dt = 0$, while $\int_0^T \sin(\omega t)^2 dt = \pi/\omega$.

For a given delay τ_1, the resulting choice between $\Delta = 0$ and $\Delta = \pi$ is the one that minimises $\cos(-\omega\tau_1 + \Delta)$, leading to the phase-shift pattern:

$$\begin{array}{ccccc} 0 & \le & \tau_1 & \le \frac{T}{4} & \Rightarrow \quad \Delta = \pi \\ \frac{T}{4} & \le & \tau_1 & \le \frac{3T}{4} & \Rightarrow \quad \Delta = 0 \\ \frac{3T}{4} & \le & \tau_1 & \le \frac{5T}{4} & \Rightarrow \quad \Delta = \pi \\ \frac{5T}{4} & \le & \tau_1 & \le \frac{7T}{4} & \Rightarrow \quad \Delta = 0 \\ & & \dots & & \end{array}$$

If the positive feedback interaction between the two oscillators is strong enough, we can reproduce this pattern. In fact, Fig. 4 shows the simulated evolution of the nonlinear system (1)–(6) in the case of identical subsystems that are oscillators when they evolve independently, with parameter values taken from the literature of segmentation clocks [3]. When the two identical oscillators are coupled by a strong enough positive feedback, the period of the oscillations is $T \approx 12$ minutes. Consistently with our theoretical expectation, when the delay is $\tau_1 = \tau_2 = 24$ minutes, namely $\frac{7T}{4} \le \tau_1 \le \frac{9T}{4}$, then $\Delta = \pi$; when the delay is $\tau_1 = \tau_2 = 30$ minutes, namely $\frac{9T}{4} \le \tau_1 \le \frac{11T}{4}$, then $\Delta = 0$; when the delay is $\tau_1 = \tau_2 = 36$ minutes, namely $\frac{11T}{4} \le \tau_1 \le \frac{13T}{4}$, then $\Delta = \pi$; when the delay is $\tau_1 = \tau_2 = 42$ minutes, namely $\frac{13T}{4} \le \tau_1 \le \frac{15T}{4}$, then $\Delta = 0$.

If the two delays τ_1 and τ_2 are not identical, the two signals will be shifted accordingly.

These alternating phase shifts have been referred to in literature as *Arnold tongue*, and have been observed in the context of entrainment of circadian rhythms [8] and coupling of synthetic oscillators [30].

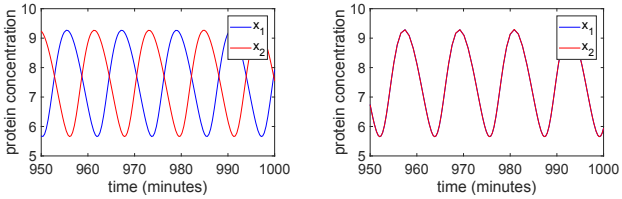

(a) $\tau_1 = \tau_2 = 24$ minutes (b) $\tau_1 = \tau_2 = 30$ minutes

(c) $\tau_1 = \tau_2 = 36$ minutes (d) $\tau_1 = \tau_2 = 42$ minutes

Fig. 4: **Simulated evolution of system** (1)–(6) with random initial conditions, $\alpha_1 = \alpha_2 = 0.4$ min^{-1}, $\beta_1 = \beta_2 = 10$ min^{-1}, $\zeta_1 = \zeta_2 = 0.11$ min^{-1}, $\varepsilon_1 = \varepsilon_2 = 0.25$ min^{-1}, $\delta_1 = \delta_2 = 0.25$ min^{-1}, $k_0 = 60$, $k_1 = 200$, $k_2 = 2 \cdot 10^{-6}$, $h = 12$. The period of the oscillations is $T \approx 12$ minutes.

V. Concluding Discussion

A delayed positive-feedback coupling between two non-homogeneous negative-feedback oscillators can have a beneficial or negative effect on the onset of oscillations: we have explained the reason and provided a condition (27), depending on the value of the delay τ and on the resonance frequency ω, to ensure that the positive-feedback interconnection favours oscillatory instability of the linearised system, thus leading to sustained oscillations. We have also given qualitative indications on the resonance frequencies of the two coupled subsystems, to facilitate oscillations.

For identical oscillators, the interconnection does not affect the onset of oscillations, but the coupling can determine whether the two oscillators are in phase or in phase opposition: we have shown that this depends on the delay and follows a precise pattern. Hence, by tuning the delay we can tune the phase shift between the two oscillatory signals.

Our results can provide useful guidelines for the design of digitally coupled single cell oscillators [10].

Most importantly, they also provide a starting point for the analysis of travelling waves in the segmentation clock, which of course are driven by coupled oscillators in many more than two cells.

Future directions include a stochastic analysis of this class of coupled oscillators. Indeed, single-cell measurements in

zebrafish embryos have revealed that the molecular components of the segmentation clock are present at low-copy numbers per cell [25]. These findings motivate a stochastic formulation and analysis of coupled genetic oscillators through a combination of Monte Carlo simulations [19], and moment closure schemes [35], [36]. Indeed, recent stochastic analysis of circadian clock models have shown trade-offs between clock precision and molecular noise [33]. As part of future work, we will tailor these results to the segmentation clock and uncover design principles for robust oscillations in spite of low-copy number noise.

Another future challenge comes from the fact that the actual segmentation-clock system always yields sustained oscillation that are in phase, despite significant changes in the parameters, including time delays. Conversely, in this paper we have shown that alternative patterns of in-phase and in-phase-opposition oscillations can arise, depending on the delay value (cf. Fig. 4). Therefore, more research is needed to reveal the additional mechanisms, not captured by the current model, that enable this biological system to exhibit *in-phase oscillations that are so extraordinarily robust* in spite of parameter variations.

REFERENCES

[1] M. J. Alam, L. Bhayana, G. R. Devi, H. D. Singh, R. B. Singh *et al.*, "Measurement of phase synchrony of coupled segmentation clocks", *Comput. Biol. Med.*, 41:916–921, 2011.

[2] A. Ay, S. Knierer, A. Sperlea, J. Holland, E. M. Özbudak, "Short-lived Her proteins drive robust synchronized oscillations in the zebrafish segmentation clock", *Development*, 140:3244–3253, 2013.

[3] A. Ay, J. Holland, A. Sperlea, G. S. Devakanmalai, S. Knierer *et al.*, "Spatial gradients of protein-level time delays set the pace of the traveling segmentation clock waves", *Development*, 141:4158–4167, 2014.

[4] N. Barkai and S. Leibler, "Circadian clocks limited by noise", *Nature*, 403:267–268, 2000.

[5] F. Blanchini, E. Franco, G. Giordano, "A Structural Classification of Candidate Oscillatory and Multistationary Biochemical Systems", *Bull. Math. Biol.*, 76(10):2542–2569, 2014.

[6] F. Blanchini, C. Cuba Samaniego, E. Franco, G. Giordano, "Design of a molecular clock with RNA-mediated regulation", *Proc. 53rd IEEE Conference on Decision and Control*, pp. 4611–4616, 2014.

[7] F. Blanchini, C. Cuba Samaniego, E. Franco, G. Giordano, "Homogeneous time constants promote oscillations in negative feedback loops", *ACS Syn. Biol.*, 7(6):1481-1487, 2018.

[8] G. Bordyugov, U. Abraham, A. Granada, P. Rose, K. Imkeller, A. Kramer, H. Herzel, "Tuning the phase of circadian entrainment", *J. Royal Soc. Interface*, 12(108), 2015.

[9] D. Bratsun, D. Volfson, L. S. Tsimring, J. Hasty, "Delay-induced stochastic oscillations in gene regulation", *PNAS*, 102(41):14 593–14 598, 2005.

[10] R. Chait, J. Ruess, T. Bergmiller, G. Tkačik, C. C. Guet, "Shaping bacterial population behavior through computer-interfaced control of individual cells", *Nature Comm.*, 8:1535, 2017.

[11] K. W. Chen, K. L. Liao, C. W. Shih, "The kinetics in mathematical models on segmentation clock genes in zebrafish", *J. Math. Biol.*, 76:97–150, 2018.

[12] C. Cuba Samaniego, G. Giordano, J. Kim, F. Blanchini, E. Franco, "Molecular titration promotes oscillations and bistability in minimal network models with monomeric regulators", *ACS Syn. Biol.*, 5(4):321–333, 2016.

[13] C. Cuba Samaniego, G. Giordano, F. Blanchini, E. Franco, "Stability analysis of an artificial biomolecular oscillator with non-cooperative regulatory interactions", *J. Biol. Dyn.*, 11(1):102–120, 2017.

[14] C. Cuba Samaniego, G. Giordano, E. Franco, "Design and analysis of a biomolecular positive-feedback oscillator", *Proc. 57th IEEE Conference on Decision and Control*, pp. 1083–1088, 2018.

[15] T. Danino, O. Mondragon-Palomino, L. Tsimring, J. Hasty, "A synchronized quorum of genetic clocks", *Nature*, 463:326–330, 2010.

[16] M. B. Elowitz and S. Leibler, "A synthetic oscillatory network of transcriptional regulators", *Nature*, 403:335–338, 2000.

[17] P. Feng and M. Navaratna, "Modelling periodic oscillations during somitogenesis", *Math. Biosci. Eng.*, 4:661, 2007.

[18] J. Ferrell, T.-C. Tsai, Q. Yang, "Modeling the cell cycle: Why do certain circuits oscillate?" *Cell*, 144(6):874 – 885, 2011.

[19] D. T. Gillespie, "Exact Stochastic Simulation of Coupled Chemical Reactions", *J. Phys. Chem.*, 81:2340–2361, 1977.

[20] B. C. Goodwin, "Oscillatory behavior in enzymatic control processes", *Adv. Enzyme Regul.*, 3:425–438, 1965.

[21] D. Gonze and W. Abou-Jaoudé, "The Goodwin model: Behind the Hill function", *PLOS ONE*, 8:1–15, 2013.

[22] N. P. Hoyle and D. Ish-Horowicz, "Transcript processing and export kinetics are rate-limiting steps in expressing vertebrate segmentation clock genes", *PNAS*, 110:E4316–E4324, 2013.

[23] A. Johnson-Buck and W. M. Shih, "Single-molecule clocks controlled by serial chemical reactions", *Nano Letters*, 17(12):7940–7944, 2017.

[24] D. J. Jörg, L. G. Morelli, F. Jülicher, "Chemical event chain model of coupled genetic oscillators", *Physical Review E*, 97:032409, 2018.

[25] S. Keskin, G. S. Devakanmalai, S. B. Kwon, H. T. Vu, Q. Hong, Y. Y. Lee, M. Soltani, A. Singh, A. Ay, E. M. Özbudak, "Noise in the vertebrate segmentation clock is boosted by time delays but tamed by notch signaling", *Cell Reports*, 23(7):2175 – 2185.e4, 2018.

[26] J.-R. Kim, D. Shin, S. H. Jung, P. Heslop-Harrison, K.-H. Cho, "A design principle underlying the synchronization of oscillations in cellular systems", *J. Cell Science*, 123:537–543, 2010.

[27] J. Lewis, "Autoinhibition with transcriptional delay: A simple mechanism for the zebrafish somitogenesis oscillator", *Current Biology*, 13:1398–1408, 2003.

[28] K. L. Liao and C. W. Shih, "A lattice model on somitogenesis of zebrafish", *Discrete Cont. Dyn. Syst. B*, 17:2789, 2012.

[29] H. P. Mirsky, A. C. Liu, D. K. Welsh, S. A. Kay, F. J. Doyle, "A model of the cell-autonomous mammalian circadian clock", *PNAS*, 106(27):11 107–11 112, 2009.

[30] O. Mondragón-Palomino, T. Danino, J. Selimkhanov, L. Tsimring, J. Hasty, "Entrainment of a population of synthetic genetic oscillators", *Science*, 333(6047):1315–1319, 2011.

[31] B. Novak and J. J. Tyson, "Design principles of biochemical oscillators", *Nat. Rev. Mol. Cell Biol.*, 9:981–991, 2008.

[32] G. Petrungaro, L. G. Morelli, K. Uriu, "Information flow in the presence of cell mixing and signaling delays during embryonic development", *Semin. Cell Dev. Biol.*, in press.

[33] W. Pittayakanchit, Z. Lu, J. Chew, M. J. Rust, A. Murugan, "Biophysical clocks face a trade-off between internal and external noise resistance", *eLife*, 7:e37624, 2018.

[34] L. Scardovi, M. Arcak, E. D. Sontag, "Synchronization of interconnected systems with applications to biochemical networks: An input-output approach", *IEEE Trans. Autom. Control*, 55(6):1367–1379, 2010.

[35] A. Singh and J. P. Hespanha, "Stochastic hybrid systems for studying biochemical processes", *Phil. Trans. Royal Soc. A*, 368:4995–5011, 2010.

[36] M. Soltani, C. A. Vargas-Garcia, A. Singh, "Conditional moment closure schemes for studying stochastic dynamics of genetic circuits", *IEEE Trans. Biomed. Circuits Syst.*, 9:518–526, 2015.

[37] T. Y. Tsai, Y. S. Choi, W. Ma, J. R. Pomerening, C. Tang, J. E. Ferrell, "Robust, tunable biological oscillations from interlinked positive and negative feedback loops", *Science*, 321:126–129, 2008.

[38] T.-L. To, M. A. Henson, E. D. Herzog, F. J. Doyle, "A molecular model for intercellular synchronization in the mammalian circadian clock", *Biophys. J.*, 92:3792–3803, 2005.

[39] K. Uriu, Y. Morishita, Y. Iwasa, "Traveling wave formation in vertebrate segmentation", *J. Theoretical Biol.*, 257:385–396, 2009.

[40] K. Uriu, Y. Morishita, Y. Iwasa, "Synchronized oscillation of the segmentation clock gene in vertebrate development", *J. Math. Biol.*, 61:207–229, 2010.

[41] Y. Wang, Y. Hori, S. Hara, F. J. Doyle III, "The collective oscillation period of inter-coupled Goodwin oscillators", *Proc. 51st IEEE Conference on Decision and Control*, pp. 1627–1632, 2012.

[42] S. Zeiser, H. V. Liebscher, H. Tiedemann, I. Rubio-Aliaga, G. K. Przemeck *et al.*, "Number of active transcription factor binding sites is essential for the Hes7 oscillator", *Theor. Biol. Med. Model.*, 3:11, 2006.